6-2008

Medium-sized double magic metal clusters: $Al@Cu_{54}^-$ and $Al@Ag_{54}^-$

Yi Gao
University of Nebraska-Lincoln, ygao3@Unl.edu

Nan Shao
University of Nebraska-Lincoln

Xiao Cheng Zeng
University of Nebraska-Lincoln, xzeng1@unl.edu

Medium-sized double magic metal clusters: $Al@Cu_{54}^-$ and $Al@Ag_{54}^-$

Yi Gao, Nan Shao, and X. C. Zeng[a)]
Department of Chemistry, University of Nebraska-Lincoln, Lincoln, Nebraska 68588, USA

(Received 4 June 2008; accepted 18 July 2008; published online 25 August 2008)

Medium-sized double magic metal clusters, $Al@Ag_{54}^-$ and $Al@Cu_{54}^-$, are predicted based on unbiased global search and density functional calculation. Both bimetallic core-shell clusters have icosahedral symmetry, and they are much lower in energies than all other low-lying isomers. In contrast, the icosahedral cluster $Al@Au_{54}^-$ is a high-energy isomer. Both $Al@Ag_{54}^-$ and $Al@Cu_{54}^-$ exhibit appreciable gaps between the highest occupied molecular orbital and the lowest unoccupied molecular orbital, and strong spherical aromaticity, which provide two additional evidences for the likelihood of their high stability. The simulated anion photoelectron spectra and optical absorption spectra are readily compared with future experiments. © *2008 American Institute of Physics*.
[DOI: 10.1063/1.2969083]

I. INTRODUCTION

Magic-number clusters are an important topic in cluster science. According to the spherical jellium model, near-spherical metal clusters with specific number of valence electrons, e.g., 8, 18, 20, 34, 40, 58,⋯, are very robust because of their closed electronic shells.[1,2] These clusters are called (electronic) magic-number clusters due to their high stability and much higher abundance in mass spectrometric studies than other sizes of metal clusters. Another hallmark of electronic magic-number clusters is that they typically have much larger energy gap between the highest occupied molecular orbital and the lowest unoccupied molecular orbital (HOMO-LUMO gap) than their neighboring-size clusters.

Besides the electronic factor, atomic packing and geometric symmetry is another important characteristic of highly stable clusters. Indeed, many known highly stable clusters exhibit very high group symmetry such as the icosahedral symmetry. Thus, highly symmetric clusters may be viewed as (geometric) magic-number clusters. The importance of both electronic and geometric factors to the stability of magic-number clusters has already been noted in previous studies.[3,4] Chen *et al.* recently proposed a viable way to design highly stable clusters based on both geometric factor (compact packing) and electronic factor (spherical aromaticity).[5] Clusters with both closed electronic shell and the icosahedral symmetry have been coined as the "double magic" clusters.[6,7] Known examples of double magic metal clusters are the icosahedral cluster I_h-Al_{13}^- (Ref. 8–13) and the core-shell clusters I_h-$W@Au_{12}$ and I_h-$Mo@Au_{12}$.[14,15] These small-sized double magic clusters possess 40 and 18 valence electrons, respectively. Clusters with both closed electronic shell and the tetrahedral symmetry may be considered as the "nearly double magic" clusters.[16] For example, the tetrahedral cluster T_d-Au_{20} (Ref. 17) possesses 20 valence electrons which form four-center two-electron bond in each of ten tetrahedral cavities. Other examples of "near-double-magic" metal clusters are the tetrahedral cluster $Sc@Cu_{16}^+$ (Ref. 18) and the core-shell cluster C_s-$Cu@Au_{16}^-$,[19] both possessing 18 valence electrons. Note that there exists a second type of double magic metal clusters, namely, group-14 Zintl ion metal clusters such as the isocahedral core-shell clusters I_h-$Al@Pb_{12}^+$ and I_h-$Pt@Pb_{12}^{2-}$ (Refs. 20 and 21) and the stannaspherene I_h-Sn_{12}^{2-} and plumbaspherene I_h-Pb_{12}^{2-}.[22,23] These small-sized metal clusters possess 50 apparent valence electrons but their high stability can be rationalized by their $5p$ and $6p$ valence band contributions which contain a total of 26 electrons[24] and obey the Wade skeletal electron rule.[25,26] The third type of double magic metal clusters was recently proposed by Dognon *et al.*,[24] namely, the 32-electron bimetallic core-shell clusters such as $Pu@Pb_{12}$ with the icosahedral symmetry.

Noble-metal clusters have been extensively studied for many years. Early experiments have established that Au_n, Ag_n, and Cu_n clusters ($n=2,8,20,34,58,\cdots$) are all electronic magic-number clusters.[27,28] In particular, gold clusters in the size range of Au_3-Au_{34} have received considerable attention.[27–39] The near-double-magic cluster T_d-Au_{20} has a very large HOMO-LUMO gap ($\Delta_{HL}=1.77$ eV).[17] For medium-sized gold clusters (with number of atoms >20), Au_{34} is an electronic magic-number cluster with a reasonably large HOMO-LUMO gap ($\Delta_{HL}=0.94$ eV) but low symmetry.[37,38] Copper and silver clusters have also been studied extensively.[40–48] In particular, the medium-sized clusters Cu_{55} and Ag_{55} are geometric magic-number clusters with the icosahedral symmetry, whereas the icosahedral cluster Au_{55} is not the global minimum.[46–49]

The bimetallic double magic cluster, I_h-$W@Au_{12}$, was first predicted by Pyykkö and Runeberg[14] and later experimentally produced and detected by Li *et al.*[15] This core-shell metal cluster has a very large HOMO-LUMO gap $\Delta_{HL}=1.68$ eV. The central "impurity" atom can be used to fine-tuning electronic properties of core-shell clusters.[50] Similar double magic clusters I_h-$M@Au_{12}^-$ ($M=V,Nb,Ta$) were also observed experimentally.[51] A number of magic-number metal clusters with 18 valence electrons have been proposed

a)Electronic mail: xczeng@phase2.unl.edu.

and studied theoretically.[52–55] These core-shell metal clusters are predicted to be stable due to the "spherical aromaticity" of the shell as well as the geometric compatibility between the shell and the core.[5]

In this paper, we report a theoretical prediction of two medium-sized double magic metal clusters of the first type, namely, the bimetallic core-shell clusters I_h-Al@M_{54}^- (M=Cu,Ag). In addition, we show that icosahedral cluster I_h-Al@Au_{54}^- is a high-energy isomer. To our knowledge, double magic metal clusters with the size greater than 20 or with valence electrons greater than 50 have not been reported previously.

II. MODELS AND METHODS

The initial structure of I_h-Al@M_{54}^- (M=Cu,Ag,Au) was constructed based on the icosahedral clusters I_h-M_{55} (M=Cu,Ag,Au), all having 42 atoms in the outer shell, 12 atoms in the inner shell, and 1 atom at the center. We simply replaced the central metal atom M by an Al atom and added a negative charge to the entire cluster so that the metal clusters possess 58 valence electrons. We then applied the basin-hopping global minimization method[56] coupled with density functional theory (DFT) (Ref. 57) to search for the lowest-energy isomer. Specifically, we used the generalized gradient approximation in the form of Perdew-Burke-Ernzerhof (PBE) functional[58] together with the double numerical plus d (DND) basis set with the semicore pseudopotential, which are implemented in the DMOL3 software package.[59,60] Harmonic frequency calculations were performed for the lowest-energy structure. The reliability of the combination of basin-hopping Monte Carlo and DFT method has been verified for the search of several highly stable metal clusters by us.[33,36,38]

Nucleus-independent chemical shift (NICS) (Refs. 61 and 62) values were computed using BP86/LAN2DZ (Refs. 63 and 64) method implemented in GAUSSIAN03 package.[65] The same level of theory was used to compute anion photoelectron spectra. The optical adsorption spectra were computed using the PBE/TZP (triple zeta polarization function) method implemented in the ADF2007 package.[66]

III. RESULTS AND DISCUSSION

The unbiased basin-hopping run generated more than 50 isomers for each of Al@M_{54}^- (M=Cu,Ag) cluster and the top-5 lowest-energy isomers of Al@M_{54}^- (M=Cu,Ag) are shown in Table I. The search suggests that the icosahedral isomer I_h-Al@M_{54}^- (M=Cu,Ag) is likely the lowest-energy structure (see 1a and 1b in Fig. 1). The second lowest-energy isomers are also displayed in Fig. 1 (2a and 2b). As shown in Table I, the second lowest-energy isomer has appreciably higher energy (>0.7 eV) than the lowest-energy isomer. This large energy difference further supports that the icosahedral structure I_h-Al@M_{54}^- (M=Cu,Ag) is most likely the *global minimum*. It is worth noting that all the top-4 lowest-lying isomers exhibit appreciable HOMO-LUMO gaps Δ_{HL} ~0.40–0.57 eV. However, for Al@Au_{54}^-, the icosahedral structure 1c is a high-energy isomer. In fact, starting from 1c, the basin-hopping run showed that within only four Monte Carlo steps the structure of 1c was changed to 2c which has a much lower energy (by 1.35 eV) than 1c. Interestingly, the core of 2c has only 11 atoms, two less than the 13-atom core of 1c. We note that the distinct structural difference between Al@Au_{54}^- and I_h-Al@M_{54}^- (M=Cu,Ag) is most likely due to the strong relativistic effect entailed in the gold cluster, as thoroughly discussed in Ref. 47.

TABLE I. (Color online) Outer shells of top-5 lowest-energy isomers of Al@Cu_{54}^- and Al@Ag_{54}^-. The core of all these isomers is I_h-Al@M_{12} (M=Cu,Ag). The energy rankings are based on PBE/DND calculation. the HOMO-LUMO gap Δ_{HL} (in unit of eV) are given in the parenthesis. ΔE is the relative energy with respect to the lowest-energy isomer.

No.	Al@Cu_{54}^-	ΔE(eV) (Δ_{HL})	Al@Ag_{54}^-	ΔE(eV) (Δ_{HL})
1	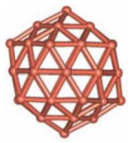	0.00 (0.43)	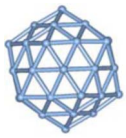	0.00 (0.40)
2	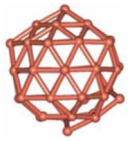	0.69 (0.57)	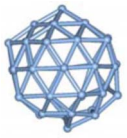	0.65 (0.53)
3	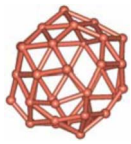	0.92 (0.54)	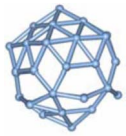	0.66 (0.54)
4	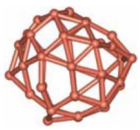	1.81 (0.52)	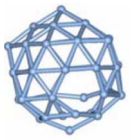	0.72 (0.53)
5	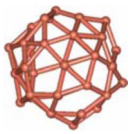	1.93 (0.56)	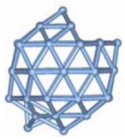	0.98 (0.17)

A. Structural, electronic, and vibrational properties

Structural, electronic, and vibrational properties of I_h-Al@Ag_{54}^- and I_h-Al@Cu_{54}^- are collected in Table II. Also included in Table II are properties of the known double magic cluster I_h-W@Au_{12} for comparison. As expected, the medium-sized clusters I_h-Al@Ag_{54}^- and I_h-Al@Cu_{54}^- have much smaller HOMO-LUMO gaps (Δ_{HL}~0.4 eV) than that (1.80 eV) for small-sized cluster I_h-W@Au_{12}. We note that Δ_{HL}~0.4 eV is close to the measured Δ_{HL}~0.65 eV of Au_{58}. The latter is an electronic magic-number cluster with 58 valence electrons.[47] I_h-Al@Au_{54}^- is a high-energy isomer but still a local minimum. The harmonic frequency calculation shows that I_h-Al@Au_{54}^- has no imaginary frequency. The lowest vibrational frequency of I_h-Al@Au_{54}^- is 19.3 cm^{-1}, much less that of I_h-Al@Ag_{54}^- (33.9 cm^{-1}) and

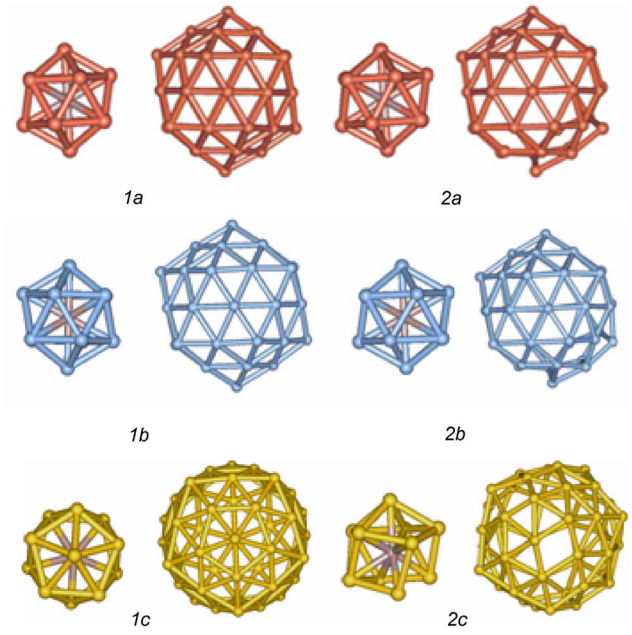

FIG. 1. (Color online) The predicted lowest-energy structure 1 and the second lowest-energy structure 2 of a Al@Cu_{54}^- and b Al@Ag_{54}^-. The inner 13-atom core and the outer 42-atom shell are plotted separately for ease of view. The Al atom (purple) is at the center of the core. 2c is an isomer of Al@Au_{54}^- with lower energy by 1.35 eV than the icosahedral isomer 1c. The core of 2c has 11 atoms.

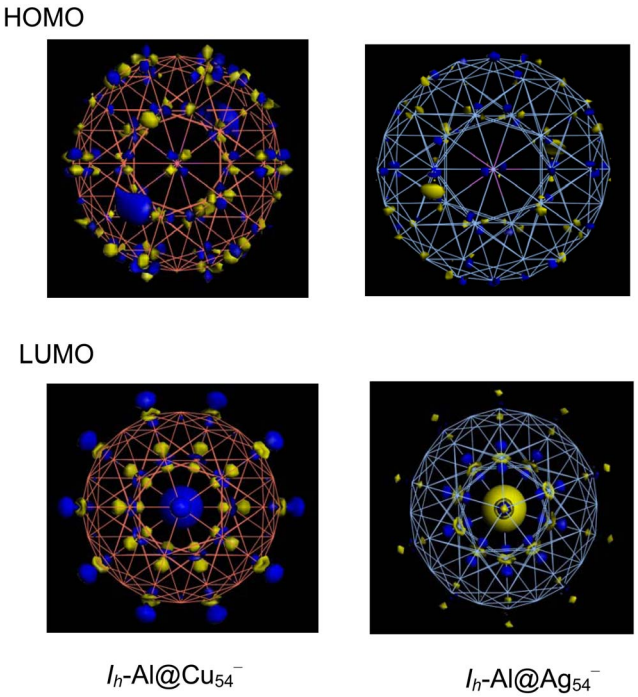

FIG. 2. (Color online) HOMO and LUMO diagrams of Al@Cu_{54}^- and Al@Ag_{54}^-. The symmetries of HOMO and LUMO are G_g and A_g, respectively.

I_h-Al@Cu_{54}^- (55.9 cm^{-1}) (Table II), indicating that I_h-Al@Ag_{54}^- and I_h-Al@Cu_{54}^- are less fluxional than I_h-Al@Au_{54}^-. This result offers an explanation that I_h-Al@Au_{54}^- may be too fluxional to maintain its icosahedral structure stable. Note that I_h-W@Au_{12}'s lowest vibrational frequency is 30.1 cm^{-1} which is also higher than that of I_h-Al@Au_{54}^-.

TABLE II. Computed properties of I_h-Al@Ag_{54}^- and I_h-Al@Cu_{54}^- vs I_h-W@Au_{12}.

	I_h-Al@Ag_{54}^-	I_h-Al@Cu_{54}^-	I_h-W@Au_{12}
Diameter (nm)	1.1	1.0	0.6
Δ_{HL} (eV)	0.40	0.43	1.80
Frontier orbital	$(h_g)^{10}(g_g)^8(a_g)^0$	$(h_g)^{10}(g_g)^8(a_g)^0$	$(t_{2g})^6(h_g)^{10}(h_g)^0$
Outer-shell longest bond (Å)	3.014	2.620	···
Outer-shell shortest bond (Å)	2.922	2.546	2.918
Inner shell (Å)	2.910	2.577	···
Al-*M* or W-Au (Å)	2.766	2.450	2.775
Lowest vibrational frequency (cm^{-1})	33.9	55.9	30.1
Highest vibrational frequency (cm^{-1})	270.3	398.1	196.9
NICS at center excluding Al or W atom	−102.6	−113.7	−56.3

B. Spherical aromaticity

Spherical aromaticity is likely an important factor to the stability of I_h-Al@Ag_{54}^- and I_h-Al@Cu_{54}^-. As shown in Table II, the NICS values at the center of 58-electron shells, I_h-Ag_{54}^{4-} and I_h-Cu_{54}^{4-}, are −102.6 and −113.7, respectively. The two NICS values are much more negative than that at the center of the 18-electron shell of I_h-Au_{12}^{6-} (−56.3), 32-electron shell I_h-Au_{32} (BP86: −80.7), and T_d-Au_{20} (BP86: −36), suggesting the stronger aromaticity for the medium-sized double magic clusters, even though the 58 valence electrons do not obey the $2(N+1)^2$ rule for spherical aromaticity. Note that the NICS value of I_h-Au_{54}^{4-} is −111.9, very close to that of I_h-Cu_{54}^{4-}, although it is not the global minimum due to strong relativistic effects.

C. HOMO and LUMO diagrams

HOMO and LUMO diagrams of I_h-Al@Ag_{54}^- and I_h-Al@Cu_{54}^- are shown in Fig. 2. It can be seen that the HOMOs are quite similar, contributed mainly by the *p* orbitals of the noble-metal atoms but little from the central Al atom. The LUMOs are mainly contributed by the *s* and *p* orbitals of noble-metal atoms as well as the 3*s* orbital of Al atom. Meanwhile, the population analysis shows that the Mülliken charges of central Al atom for I_h-Al@Ag_{54}^- and I_h-Al@Cu_{54}^- are 1.82*e* and 2.99*e*, respectively. More interestingly, the negative charges for middle-shell and outer-shell present different trend for the two clusters. For I_h-Al@Ag_{54}^-, each Ag atom in the middle shell possesses a

charge of −0.048*e*, slightly less negative than that of the outer shell (vertex: −0.051*e*; edge: −0.055*e*). While for I_h-Al@Cu_{54}^-, each Cu atom in the middle shell possesses −0.144*e*, more negative than that of the outer shell (vertex: −0.051*e*; edge: −0.055*e*). Note also that for both clusters, the Mülliken charges of the outer surface are almost same (I_h-Al@Ag_{54}^-: −2.24*e*; I_h-Al@Cu_{54}^-: −2.27*e*), suggesting that both clusters have very similar electronic properties.

D. Simulated anion photoelectron spectra

Simulated anion photoelectron spectra of I_h-Al@Ag_{54}^- and I_h-Al@Cu_{54}^-, together with the simulated spectrum of I_h-Ag_{55}^- are shown in Fig. 3. The I_h-Ag_{55}^- is known to be the global minimum of Ag_{55}^- and the experimental photoelectron spectrum of I_h-Ag_{55}^- has been reported previously.[46] In the photoelectron spectrum, the location of the first peak characterizes the vertical detachment energies of the anion, which are ~3.1 eV for I_h-Al@Ag_{54}^- and I_h-Ag_{55}^- and ~3.0 eV for I_h-Al@Cu_{54}^-. The gap between the first two peaks gives rise to the HOMO1-HOMO2 gaps of the clusters, which are 0.68 eV for I_h-Al@Cu_{54}^-, 0.70 eV for I_h-Al@Ag_{54}^-, and 0.62 eV for I_h-Ag_{55}^-. Additionally, the photoelectron spectrum of I_h-Al@Ag_{54}^- and I_h-Ag_{55}^- exhibits the same sequence of the group symmetry for the first five peaks, suggesting that the replacement of the central Ag atom by Al in I_h-Ag_{55}^- does not change the order of the occupied orbitals, even though the orbital energies are changed [as can be seen in Fig. 3 that the third (T_{1u}) and fourth (G_u) peaks nearly overlap with each for I_h-Al@Ag_{54}^-].

E. Computed optical absorption spectra

Computed optical absorption spectra (less than 4 eV) of I_h-Al@Ag_{54}^- and I_h-Al@Cu_{54}^- are shown in Fig. 4. Unlike the photoelectron spectra, the two optical spectra are quite different. For Al@Ag_{54}^-, there are two weak peaks at 1.70 and 1.86 eV, one modest peak at 2.33 eV, and a strong peak at 2.65 eV. There are no apparent absorption peaks between 3 and 4 eV. However, for Al@Cu_{54}^-, there is one modest peak at ~1.52 eV, one very strong peak at ~2.0 eV, and one modest peak between 3 and 4 eV.

Finally, we note that besides I_h-Al@Ag_{54}^- and I_h-Al@Cu_{54}^- we have performed structural optimization (using PBE/DND level of theory) for a series of bimetallic core-shell clusters I_h-$M@N_{54}^{\delta}$ (M=Pb,Sn,Zr,Ti,Sc,V,Ce,Th; N=Ag,Cu; δ=−1,0,+1), all having 58 valence electrons. It is found that only I_h-Ti@Ag_{54}, I_h-Zr@Ag_{54}, I_h-Ti@Cu_{54}, I_h-Zr@Cu_{54}, I_h-Th@Ag_{54}, I_h-Th@Cu_{54}, I_h-Sc@Ag_{54}^-, and I_h-Sc@Cu_{54}^- can be optimized successfully, and these clusters show smaller HOMO-LUMO gaps (Δ_{HL} ~0.06–0.32 eV) than the isoelectronic clusters I_h-Al@Ag_{54}^- and I_h-Al@Cu_{54}^-. The latter two have larger HOMO-LUMO gaps because their 58 valence electrons are composed of doubly occupied *s* and *p* shells and singly occupied *d*, *f*, and *g* shells. Thus, the inner atom is more likely to be a simple *sp* atom (e.g., Al) which can strongly attract *s* and *p* electrons. Unbiased searches are needed to further confirm that these icosahedral core-shell clusters are the global minima, i.e., double magic metal clusters. Nevertheless, the preliminary result suggests that the actinides seem capable of maintaining the clusters at the highest icosahedral symmetry, but the lanthanides seem not.[24]

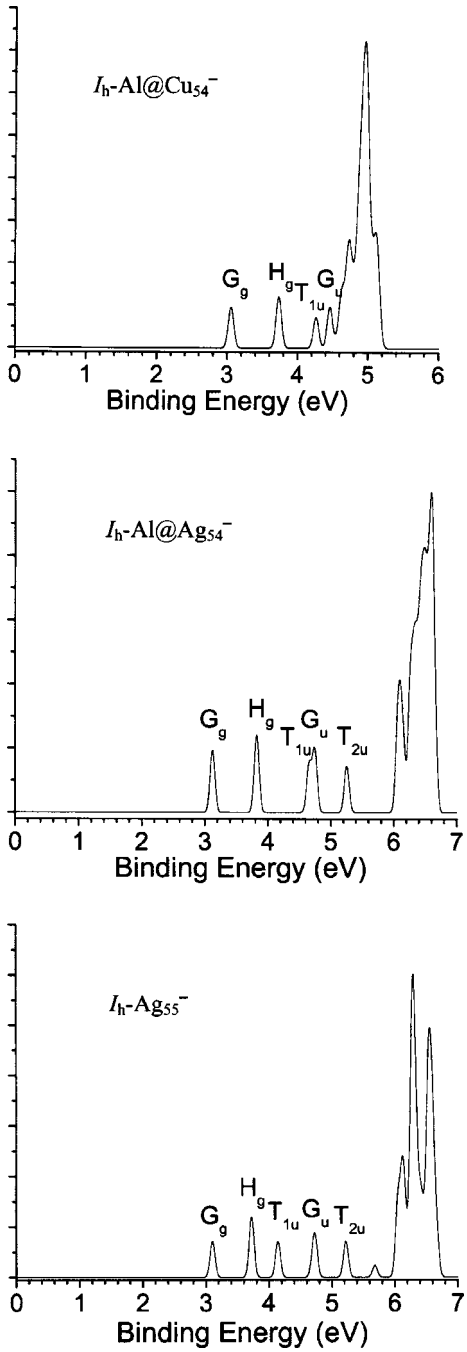

FIG. 3. Simulated anion photoelectron spectra of I_h-Al@Cu_{54}^-, I_h-Al@Ag_{54}^-, and I_h-Ag_{55}^-, based on BP86/LANL2DZ level of theory implemented in GAUSSIAN03 program (Ref. 65).

IV. CONCLUSION

In conclusion, we present theoretical evidence of two medium-sized double magic metal clusters I_h-Al@Ag_{54}^- and I_h-Al@Cu_{54}^-. The unbiased search shows that the icosahedral isomer is markedly lower in energy than other low-lying isomers. Both I_h-Al@Ag_{54}^- and I_h-Al@Cu_{54}^- have appreciable HOMO-LUMO gaps. Moreover, the isoelectronic

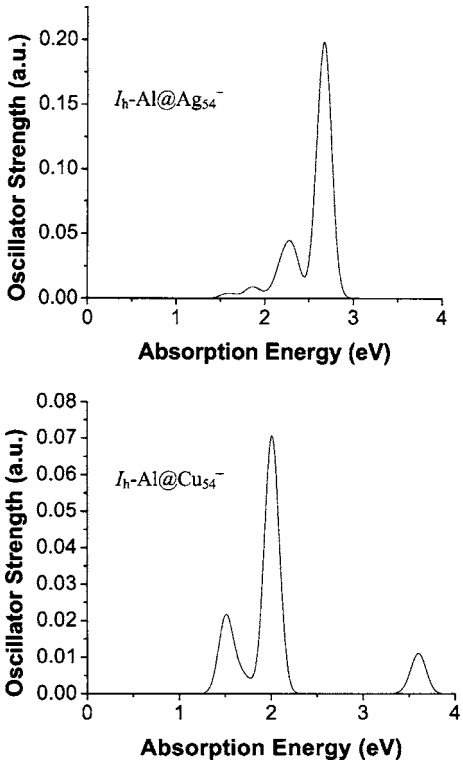

FIG. 4. Simulated optical absorption spectra of Al@Ag_{54}^- and Al@Cu_{54}^- based on the time-dependent DFT method at PBE/TZP level of theory implemented in the ADF program (Ref. 66).

outer shells I_h-Ag_{54}^{4-} and I_h-Cu_{54}^{4-} exhibit very large negative NICS values at their center, significantly more negative than other known double magic metal clusters. This result suggests that both I_h-Al@Ag_{54}^- and I_h-Al@Cu_{54}^- entail strong spherical aromaticity which may contribute to the stabilization of the icosahedral structure. The calculated anion photoelectron spectra as well as the optical absorption spectra of I_h-Al@Ag_{54}^- and I_h-Al@Cu_{54}^- are ready to compare with measured spectra in future. Finally, since I_h-Ag_{55}^- and I_h-Cu_{55}^- are stable at room temperature,[46] we expect that I_h-Al@Ag_{54}^- and I_h-Al@Cu_{54}^- are likely to be stable at the room temperature too. At elevated temperatures, however, isomers with lower symmetry would be more stable due to entropy effect. It will be interesting to find out the temperature at which the structural transition occurs. This study will be carried out in future.

ACKNOWLEDGMENTS

This work was supported by grants from NSF (CHE and CMMI), the Nebraska Research Initiative, and by the Research Computing Facility at University of Nebraska-Lincoln and Peter Kiewit Institute's Holland Computing Center at University of Nebraska-Omaha.

[1] W. D. Knight, K. Clemenger, W. A. de Heer, W. A. Saunders, M. Y. Chou, and M. L. Cohen, Phys. Rev. Lett. **52**, 2141 (1984).
[2] W. A. de Heer, Rev. Mod. Phys. **65**, 611 (1993).
[3] S. N. Khanna and P. Jena, Phys. Rev. Lett. **69**, 1664 (1992).
[4] P. v. R. Schleyer and A. I. Boldyrev, J. Chem. Soc., Chem. Commun., 1536 (1991).
[5] Z. Chen, S. Neukermans, X. Wang, E. Janssens, Z. Zhou, R. E. Silverans, R. B. King, P. v. R. Schleyer, and P. Lievens, J. Am. Chem. Soc. **128**, 12829 (2006).
[6] T. P. Martin, Phys. Rep. **273**, 199 (1996).
[7] Z. Chen and R. B. King, Chem. Rev. (Washington, D.C.) **105**, 3613 (2005).
[8] R. E. Leuchtner, A. C. Harms, and A. W. Castleman, Jr., J. Chem. Phys. **91**, 2753 (1989).
[9] A. C. Harms, R. E. Leuchtner, S. W. Sigsworth, and A. W. Castleman, Jr., J. Am. Chem. Soc. **112**, 5673 (1990).
[10] B. T. Cooper, D. Parent, and S. W. Buckner, Chem. Phys. Lett. **284**, 401 (1998).
[11] S. N. Khanna and P. Jena, Phys. Rev. B **51**, 13705 (1995).
[12] B. K. Rao and P. Jena, J. Chem. Phys. **111**, 1890 (1990).
[13] D. E. Bergeron, A. W. Castleman, Jr., T. Morisato, and S. N. Khanna, Science **304**, 84 (2004).
[14] P. Pyykkö and N. Runeberg, Angew. Chem., Int. Ed. **41**, 2174 (2002).
[15] X. Li, B. Kiran, J. Li, H.-J. Zhai, and L.-S. Wang, Angew. Chem., Int. Ed. **41**, 4786 (2002).
[16] R. B. King, Z. Chen, and P. v. R. Schleyer, Inorg. Chem. **43**, 4564 (2004); M. P. Johansson and P. Pyykkö, Phys. Chem. Chem. Phys. **6**, 2907 (2004).
[17] J. Li, X. Li, H. J. Zhai, and L. S. Wang, Science **299**, 864 (2003).
[18] N. Veldeman, T. Höltzl, S. Neukermans, T. Veszprémi, M. T. Nguyen, and P. Lievens, Phys. Rev. A **76**, 011201 (2007).
[19] L.-M. Wang, S. Bulusu, H.-J. Zhai, X. C. Zeng, and L.-S. Wang, Angew. Chem., Int. Ed. **46**, 2915 (2007).
[20] S. Neukermans, E. Janssens, Z. F. Chen, R. E. Silverans, P. v. R. Schleyer, and P. Lievens, Phys. Rev. Lett. **92**, 163401 (2004).
[21] E. N. Esenturk, J. Fettinger, Y.-F. Lam, and B. Eichhorn, Angew. Chem., Int. Ed. **43**, 2132 (2004).
[22] L. F. Cui, X. Huang, L. M. Wang, D. Y. Zubarev, A. I. Boldyrev, J. Li, and L. S. Wang, J. Am. Chem. Soc. **128**, 8390 (2006).
[23] L. F. Cui, X. Huang, L. M. Wang, J. Li, and L. S. Wang, J. Phys. Chem. A **110**, 10169 (2006).
[24] J.-P. Dognon, C. Clavaguera, and P. Pyykkö, Angew. Chem., Int. Ed. **46**, 1427 (2007).
[25] K. Wade, J. Chem. Soc., Chem. Commun., 792 (1971).
[26] K. Wade, Adv. Inorg. Chem. Radiochem. **18**, 1 (1976).
[27] I. Katakuse, T. Ichihara, Y. Fujita, T. Matsuo, T. Sakurai, and H. Matsuda, Int. J. Mass Spectrom. Ion Process. **67**, 229 (1985).
[28] A. Herlert, S. Krückeberg, L. Schweikhard, M. Vogel, and C. Walther, J. Electron Spectrosc. Relat. Phenom. **106**, 179 (2000).
[29] H. Häkkinen and U. Landman, Phys. Rev. Lett. **62**, R2287 (2000).
[30] F. Furche, R. Ahlrichs, P. Weis, C. Jacob, S. Glib, T. Bierweiler, and M. M. Kappes, J. Chem. Phys. **117**, 6982 (2002).
[31] H. Häkkinen, B. Yoo, U. Landman, X. Li, H.-J. Zhai, and L.-S. Wang, J. Phys. Chem. A **107**, 6168 (2003).
[32] M. Ji, X. Gu, X. Li, X. G. Gong, J. Li, and L.-S. Wang, Angew. Chem., Int. Ed. **44**, 7119 (2005).
[33] S. Bulusu, X. Li, L.-S. Wang, and X. C. Zeng, Proc. Natl. Acad. Sci. U.S.A. **103**, 8326 (2006).
[34] X. Xing, B. Yoon, U. Landman, and J. H. Parks, Phys. Rev. B **74**, 165423 (2006).
[35] B. Yoon, P. Koskinen, B. Huber, B. Kostko, B. v. Issendorff, H. Häkkinen, M. Moseler, and U. Landman, ChemPhysChem **8**, 157 (2007).
[36] S. Bulusu, X. Li, L.-S. Wang, and X. C. Zeng, J. Phys. Chem. C **111**, 4190 (2007).
[37] A. Lechtken, D. Schooss, J. R. Stairs, M. N. Blom, F. Furche, N. Morgner, O. Kostko, B. von Issendorff, and M. M. Kappes, Angew. Chem., Int. Ed. **46**, 2944 (2007).
[38] X. Gu, S. Bulusu, X. Li, X. C. Zeng, J. Li, X. G. Gong, and L. S. Wang, J. Phys. Chem. C **111**, 8228 (2007).
[39] P. D. Jadzinsky, G. Calero, C. J. Ackerson, D. A. Bushnell, and R. D. Kornberg, Science **318**, 430 (2007).
[40] M. N. Blom, D. Schooss, J. Stairs, and M. M. Kappes, J. Chem. Phys. **124**, 244308 (2006).
[41] M. Yang, K. A. Jackson, and J. Jellinek, J. Chem. Phys. **125**, 144308 (2006).
[42] R. Fournier, J. Chem. Phys. **115**, 2165 (2001).
[43] M. Yang, K. A. Jackson, C. Koehler, T. Frauenheim, and J. Jellinek, J. Chem. Phys. **124**, 024308 (2006).
[44] B. C. Longo and L. J. Gallego, Phys. Rev. B **74**, 193409 (2006).
[45] D. Tian, H. Zhang, and J. Zhao, Solid State Commun. **144**, 174 (2007).
[46] H. Häkkinen, M. Moseler, O. Kostko, N. Morgner, M. A. Hoffmann, and

B. v. Issendorff, Phys. Rev. Lett. **93**, 093401 (2004).
[47] W. Huang, M. Ji, C.-D. Dong, X. Gu, L.-M. Wang, X. G. Gong, and L.-S. Wang, ACS Nano **2**, 897 (2008); see also http://pubs.acs.org/journals/ancac3/index.html
[48] X. Xing, R. M. Danell, I. L. Garzón, K. Michaelian, M. N. Blom, M. M. Burns, and J. H. Parks, Phys. Rev. B **72**, 081405 (2005).
[49] D. R. Jennison, P. A. Schultz, and M. P. Sears, J. Chem. Phys. **106**, 1856 (1997).
[50] P. Schwerdtfeger, Angew. Chem., Int. Ed. **42**, 1892 (2003).
[51] H.-J. Zhai, J. Li, and L.-S. Wang, J. Chem. Phys. **121**, 8369 (2004).
[52] Y. Gao, S. Bulusu, and X. C. Zeng, J. Am. Chem. Soc. **127**, 15680 (2005).
[53] Y. Gao, S. Bulusu, and X. C. Zeng, ChemPhysChem **7**, 2275 (2006).
[54] R. J. H. Xie, C. F. Cheung, and J. J. Zhao, J. Comput. Theor. Nanosci. **3**, 312 (2006).
[55] K. Manninen, P. Pyykkö, and H. Häkkinen, Phys. Chem. Chem. Phys. **7**, 2208 (2005).
[56] D. J. Wales and H. A. Scheraga, Science **285**, 1368 (1999).
[57] S. Yoo and X. C. Zeng, Angew. Chem., Int. Ed. **44**, 1491 (2005).
[58] J. P. Perdew, K. Burke, and M. Ernzerhof, Phys. Rev. Lett. **77**, 3865 (1996).
[59] B. Delley, J. Chem. Phys. **92**, 508 (1990).
[60] B. Delley, J. Chem. Phys. **113**, 7756 (2000).
[61] P. v. R. Schleyer, C. Maerker, A. Dransfeld, H. Jiao, and N. J. R. v. E. Hommes, J. Am. Chem. Soc. **118**, 6317 (1996).
[62] Z. Chen, C. S. Wannere, C. Corminboeuf, R. Puchta, and P. v. R. Schleyer, Chem. Rev. (Washington, D.C.) **105**, 3842 (2005).
[63] A. D. Becke, Phys. Rev. A **38**, 3098 (1988).
[64] J. P. Perdew, Phys. Rev. B **33**, 8822 (1986).
[65] M. J. Frisch, G. W. Trucks, H. B. Schlegel *et al.*, GAUSSIAN03, Revision C.02, Gaussian, Inc., Wallingford, CT, 2004.
[66] ADF 2007.01, SCM, Theoretical Chemistry, Vrije Universiteit, Amsterdam, The Netherlands (http://www.scm.com).